Corrosion inhibition of steel in acidic solution using *p*-bromopiperazinylbenzene: Experimental and DFT calculations

A.F. Mahmood,¹ H.S. Aljobori,² H.H. Al-Doori,³ F.F. Sayyid,⁴ A.M. Mustafa,⁴ A.A.H. Kadhum⁵ and A. Alamiery⁶*

¹Oil and Gas Engineering Department/University of Technology, Baghdad, P.O. Box: 10001, Baghdad, Iraq

²College of Engineering, University of Warith Al-Anbiyaa, P.O. Box: 56001, Karbalaa, Iraq

³Al-Karkh University of Science, P.O. Box: 10001, Baghdad, Iraq ⁴Production and Metallurgy Engineering Department, University of Technology-Iraq, P.O. Box: 10001, Baghdad, Iraq

⁵Faculty of Medicine, University of Al-Ameed, P.O. Box: 56001, Karbala, Iraq ⁶Al-Ayen Scientific Research Center, Al-Ayen Iraqi University, AUIQ, An Nasiriyah, P.O. Box: 64004, Thi Qar, Iraq

*E-mail: dr.ahmed1975@gmail.com

Abstract

This study investigates the corrosion inhibition efficiency of *para*-bromopiperazinylbenzene (PBPB) for mild steel in an acidic medium using weight loss methods at various concentrations (0.1 to 0.5 mM) and immersion time of 5 hours. The inhibition efficiency was found to increase with the inhibitor concentration, reaching a maximum efficiency of 91.3% at the highest concentration. The effect of temperature on corrosion inhibition was also studied at 303 K, 313 K, 323 K, and 333 K, showing a slight increase in inhibition efficiency with rising temperature. Potentiodynamic polarization measurements were conducted at 303 K, confirming the trend observed in weight loss studies. Adsorption isotherm analysis revealed that the inhibitor obeys the Langmuir adsorption isotherm, with the free energy of adsorption suggesting a combination of chemisorption and physisorption processes. Density Functional Theory (DFT) calculations were performed to study the quantum chemical parameters such as $E_{\rm HOMO}$, $E_{\rm LUMO}$, and others, showing good correlation with experimental data. The harmony between experimental and theoretical results underscores the potential of PBPB as an effective corrosion inhibitor for mild steel in acidic environments.

Received: December 4, 2024. Published: May 19, 2025 doi: 10.17675/2305-6894-2025-14-2-15

Keywords: corrosion inhibition, para-bromopiperazinylbenzene, mild steel, acidic medium, DFT analysis.

1. Introduction

Corrosion is a pervasive issue in various industries, leading to significant economic losses and safety concerns. It is one of the natural electrochemical processes happening in metals, such as ordinary carbon steel, creating harmful environmental spoilage over time and structural members' failures. Mild steel is widely used in various industries such as construction. automotive, oil, gas, etc., but is much susceptible to corrosion under acidic content [1, 2]. Hydrochloric acid (HCl) is one among those acids widely used for industrial processes, like pickling, de-scalement, and acidizing of oil wells, and is very aggressive towards mild steel. this conditioning too is well mitigated by using corrosion inhibitors to cover the metal surface and elongate the lifetime of equipment used [3]. Inhibitors prevent corrosion when they are present in trace amounts and mainly involve the two categories: organic and inorganic. Some inorganic inhibitors are chromates, nitrates, and phosphates, which are highly efficient but have disadvantages, including toxic and environmental hazards with harmful by-products formed [4]. On the other hand, organic inhibitions not only perform well but also generate interest among researchers with bio-disposability and environmentally friendliness due to the adsorptive ability of creating a protective layer on the metal surface that inhibits corrosion [5]. Such heteroatoms in these inhibitors include nitrogen, oxygen, and sulfur, enhancing the tendency of the compounds to interact with metal surfaces either by donating or accepting electrons [6]. This means that the strong interaction between organic inhibitors and metal surfaces will result in stable adsorbing layers preventing further corrosion. Organic inhibitors appear to be multifunctional and can be designed to be optimal for particular corrosion types combined with environmental conditions [7]. Attention has spread from corrosion studies under other environments to the scenario of a well-studied environment, hydrochloric acid in the industry. Mild steel is corrosion prone; inhibit it using corrosion inhibitors; especially organic inhibitors because they have proved to be the most favorable. Although such efficacious inorganic inhibitors as chromates are always used, they have limits due to their carcinogenicity and environmental risks. Phosphates limit use for less toxicity but are a major contributor to the eutrophication of aquatic systems. Organic inhibitors are, thus, less toxic, more biodegradable, and able to form sulfonate protective barriers through functional groups containing nitrogen, oxygen, or sulfur. The efficiency can be improved through molecular optimization and concentration [12, 13].

Density Functional Theory (DFT) advances have brought forth organic inhibitors. Indeed, DFT goes a long way in describing molecular interaction character with metal surfaces by such electronic properties as highest occupied molecular orbital (HOMO), lowest unoccupied molecular orbital (LUMO), and dipole moment. Such molecules have higher HOMO energies and lower energy levels for LUMO, thus making them better in inhibition efficiency because of easy donation of electrons to form strong protective layers [14]. *para*-substituted organic compounds, have been reported to be excellent corrosion inhibitors. Benzene ring with bromine as a substituent along with a pyrrolidine moiety is N-

TBI. Its structure has an importance because it contains electron-withdrawing bromine like the electron-donating piperazine and brings about electron distribution, reactivity, and interaction with metal surfaces to be of the effective corrosion inhibitors. The combination of these substituents contributes much toward its effectiveness as corrosion inhibitor. N-TBI is found to be effective in acid conditions as a corrosion inhibitor of steel, providing economic and ecological benefits in cut down maintenance costs and impact on the environment [15]. Incorporating the bromine atom in its molecular framework alters the electronic properties of PBPB so that it increases the adsorption capacity or strength and interaction with metal surfaces. PBPB is likely to provide long-term protection against corrosion through combination of chemisorption and physisorption as indicated by preliminary studies [15, 16]. The present investigation seeks to continue previous research efforts to establish the ability of PBPB to protect mild steel in acidic medium. In addition, the study augments existing knowledge on effective inhibitors by coupling experimental techniques-such as weight loss measurements and potentiodynamic polarization-with DFT calculations toward a more comprehensive understanding of PBPB's performance and mechanisms. The outcome will have a significant impact on the development of efficient, environmentally friendly corrosion inhibitors for industrial applications.

Figure 1. The chemical structure of PBPB.

2. Materials and Methods

2.1. Materials

Company of Metal Samples was the supplier for mild steel coupons which were employed as the working electrodes in this investigation. The chemical composition of the mild steel coupons, expressed in weight percentage, is detailed in Table 1. Prior to experimentation, the mild steel coupons were cleaned according to the standard method G1-03/ASTM [16, 17].

Table 1. Chemical composition of mild steel coupons (wt.%).

Element	Carbon	Manganese	Silicon	Aluminum	Sulfur	Phosphorus	Iron
Percentage	0.210	0.050	0.380	0.010	0.050	0.090	Balance

2.2. Preparation of acidic solution

The corrosive solution was prepared by diluting 37% HCl (Merck-Malaysia) with distilled water.

2.3. Weight loss measurements

Weight loss experiments were conducted at time intervals of 1, 6, 12, 24, and 48 hours, across temperatures ranging from 303 K to 333 K. Mild steel coupons were exposed to inhibitor concentrations of 0, 0.1, 0.2, 0.3, 0.4, 0.5, and 1 mM. Following exposure, the mild steel specimens were carefully cleaned with distilled water and acetone, dried in an oven, and weighed. Measurements were conducted in triplicate, and the mean weight loss values were determined [18]. The corrosion rate (C_R) in mm/year and inhibition efficiency (IE) were determined using Equations (1) and (2):

$$C_{\rm R} = \frac{87600 \times W}{a \times t} \tag{1}$$

where W represents the weight loss of the tested mild steel (grams), a denotes the surface area of the tested mild steel (cm 2), and t represents the exposure time in hours.

$$IE\% = \frac{C_{R(0)} - C_{R(i)}}{C_{R(0)}} \times 100$$
 (2)

where $C_{R(0)}$ represents the corrosion rate in the absence of the inhibitor, and $C_{R(i)}$ represents the corrosion rate in the presence of the inhibitor.

2.4. Potentiodynamic polarization measurements

Potentiodynamic polarization measurements were conducted in a 1.0 M HCl solution with varying concentrations of PBPB as the corrosion inhibitor. The experiments were performed using a Gamry Instrument Potentiostat/Galvanostat/ZRA (REF 600) model, equipped with a water-jacketed glass cell containing three electrodes: a working electrode (mild steel specimen), a counter electrode (graphite rod), and a reference electrode (saturated calomel electrode, SCE). The working electrode was prepared by polishing, thoroughly cleaning, and immersing it in the test solution until a stable open-circuit potential (OCP) was achieved, typically within 30 minutes of immersion [19]. Potentiodynamic polarization curves were recorded by varying the potential from -250 mV to +250 mV relative to the OCP at a scan rate of 0.5 mV/s. The corrosion current density (i_{corr}) and corrosion potential (E_{corr}) were derived from the Tafel extrapolation method using Gamry's DC105 software. The inhibition efficiency was determined by comparing the i_{corr} values in the absence and presence of the inhibitor. To ensure reliability, all measurements were performed in triplicate, and the average values were reported. These tests provided valuable information on the anodic and cathodic reactions occurring on the mild steel surface in the acidic medium, offering insights into the inhibition mechanism of PBPB.

2.5. Density Functional Theory (DFT) computations

Quantum chemical computations were performed to complement experimental findings. Gaussian 03 software was utilized for the DFT calculations. Becke's three-parameter hybrid

functional (B3LYP) level with the Gaussian 03 version [20], employing the 6–31G reference set, was employed to investigate the chemical reactivity of the PBPB molecule. Quantum parameters including energy gap (ΔE), fraction of electron transfer (ΔN), dipole moment (μ), ionization energy (I), electron affinity (A), absolute electronegativity (χ), hardness (η), and softness (σ) were determined for PBPB in the gas phase [21]. The quantum chemical parameters were calculated using Equations (3–8):

$$I = -E_{\text{HOMO}} \tag{3}$$

$$A = -E_{\text{LUMO}} \tag{4}$$

$$\chi = \frac{I + A}{2} \tag{5}$$

$$\eta = \frac{I - A}{2} \tag{6}$$

$$\sigma = \frac{1}{\eta} \tag{7}$$

$$\Delta N = \frac{\chi_{\text{Fe}} - \chi_{\text{inh}}}{2(\eta_{\text{Fe}} + \eta_{\text{Fe}})} \tag{8}$$

where γ_{Fe} is the electronegativity of iron and η_{inh} is the hardness of iron.

The conceptually correct way to calculate ΔN for interactions between a molecule and a metal surface requires the use of the metal's work function rather than the free electron gas Fermi energy. $\chi_{\text{Fe}}=U_{\text{Fe}}$, the work function of iron ($U_{\text{Fe}}=4.5 \text{ eV}$) [22].

3. Results and Discussion

The effectiveness of corrosion inhibitors is typically evaluated by analyzing their ability to reduce the corrosion rate of metals in aggressive environments. In the current investigation, the PBPB performance as corrosion inhibition for mild steel in a 1.0 M HCl was studied using weight loss techniques and potentiodynamic polarization measurements. The above approach utilizes the concentration of inhibitor and temperature to evaluate results within the purview of interactions of PBPB molecules and the mild steel surface. The detailed process that highlights the mechanism of inhibition will then follow this. Initially, the effect of several concentrations of inhibitor with regard to the corrosion rate and the inhibition efficiency is considered, specifically explaining how the inhibitor forms protective layers thereby practically minimizing the corrosive impact arising from hydrochloric acid. This will be followed by temperature on which the inhibition was done; it will, thus, provide light on the aspects of the factors affecting stability and adsorption patterns of PBPB under varying thermal conditions. Potentiodynamic polarization data also discuss those anodic and cathodic reactions that comprise the inhibition mechanism. Adsorption isotherms and quantum chemical calculations are also incorporated to provide a theoretical interpretation of the empirical observations. A comprehensive approach like this provides a deeper understanding of inhibition mechanisms, particularly regarding efficacy and thermal stability as a corrosion inhibitor for use in industrial applications involving mild steel in an acidic environment. This is shown in Figure 2, where the corrosion rate (C_R) and inhibition efficiency (IE%) of PBPB in mild steel in 1.0 M HCl are shown in relation with different concentrations of the inhibitor (0.1–0.5 mM) and temperature (303 K, 313 K, 323 K, and 333 K). These were determined through weight loss techniques over a period of five hours in contact.

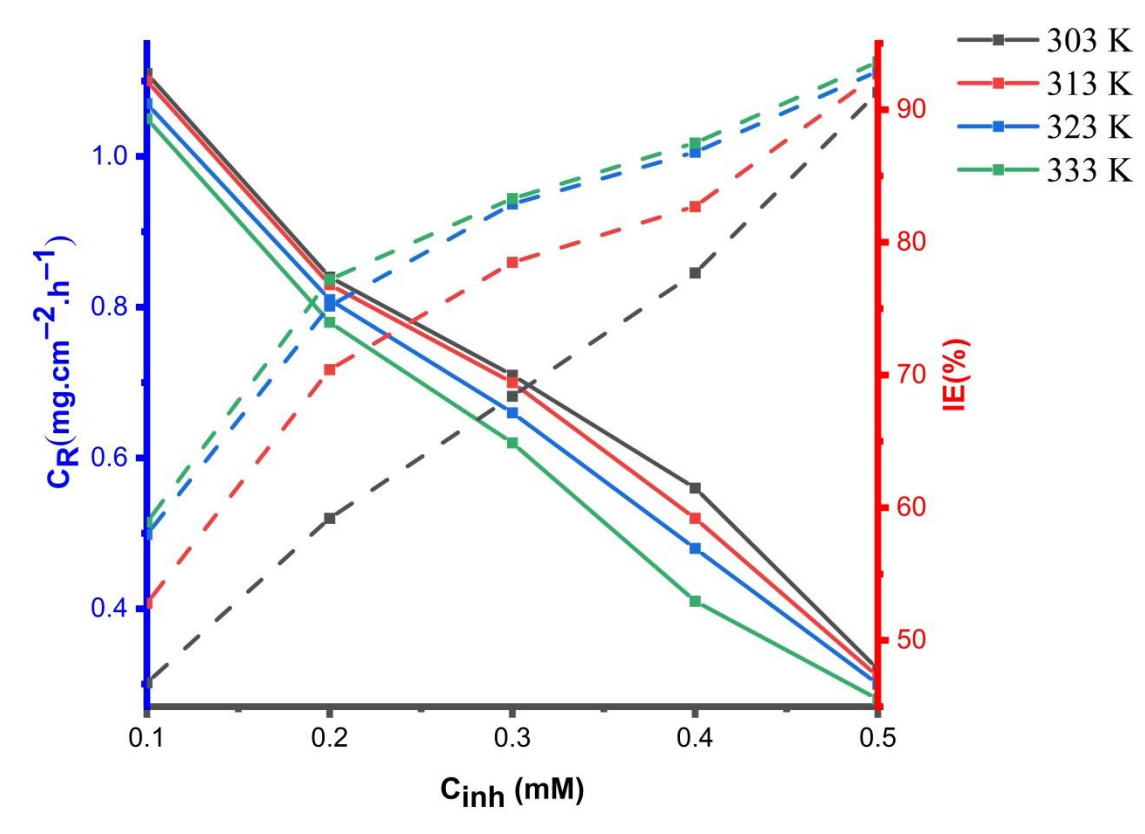


Figure 2. C_R and IE% of mild steel in 1.0 M HCl as a function of PBPB concentration at various temperatures for an immersion period of 5 hours.

3.1. Weight loss measurements

3.1.1. Effect of inhibitor concentration

As shown in Figure 2, the corrosion rate of mild steel decreases as the concentration of PBPB increases across all studied temperatures. At a low concentration of 0.1 mM, the corrosion rate remains relatively high, indicating insufficient surface coverage by the inhibitor. However, with higher concentrations, the corrosion rate decreases steadily, demonstrating improved protection due to enhanced surface coverage by PBPB molecules [24]. Similarly, the inhibition efficiency increases with rising inhibitor concentration, reflecting the formation of a protective layer on the mild steel surface that effectively blocks the interaction with the acidic medium. At the highest concentration of 0.5 mM, the inhibition efficiency

peaks at approximately 91.3%, confirming the inhibitor's strong protective performance at adequate concentrations.

3.1.2. Effect of temperature

The influence of temperature on inhibition efficiency was examined within the range of 303 K to 333 K. As seen in Figure 2, inhibition efficiency increases slightly with temperature across all concentrations of PBPB, particularly at higher concentrations. At 303 K, inhibition efficiency is already significant but improves marginally as the temperature rises to 313 K, 323 K, and 333 K. This trend indicates that PBPB adsorption involves both physisorption and chemisorption, with the chemisorption component strengthening at elevated temperatures. The combined adsorption mechanisms contribute to maintaining a superior performance of the inhibitor at high temperatures because it is stable and effective even when used in industrial conditions where the heat is hiked [25]. In summary, Figure 2 illustrates how PBPB can be used as a corrosion inhibitor against mild steel when it is exposed to acidic environments. The inhibitory efficiency increases with increasing concentrations of the inhibitor, but the highest inhibition efficiency was recorded at 91.3% for 0.5 mM concentrations of the inhibitor at 333 K [30]. This development implies that PBPB is another example of cost-effective and effective corrosion inhibitor applicable to protecting corrosion on equipment used in various types of industrial activities.

3.2. Potentiodynamic polarization measurements

Curves of potentiodynamic polarization of mild steel in 1 M HCl solution with the various concentrations of PBPB are depicted in Figure 3, and the tabulation of Tafel polarization was provided at I217. Parameter such as $E_{\rm corr}$, anodic Tafel slope, cathodic Tafel slope, $i_{\rm corr}$, $C_{\rm R}$ and IE% are included [26]. A graphical representation of the electrochemical behavior of mild steel in an acidic environment due to PBPB concentration has been discussed and photo-graphed in Figure 3. The blank solution (0.0 mM, black) exhibits the highest current density, indicative of significant corrosion. As PBPB concentration increases, the curves shift towards lower current densities, signaling a reduction in both anodic and cathodic reactions. This implies that PBPB may provide a double mechanism of action as a corrosion inhibitor by inhibiting both the anodic dissolution of iron and the cathodic hydrogen evolution reaction. Thus, PBPB acts as a mixed-type inhibitor, suppressing both electrochemical reactions related to corrosion concurrently [27].

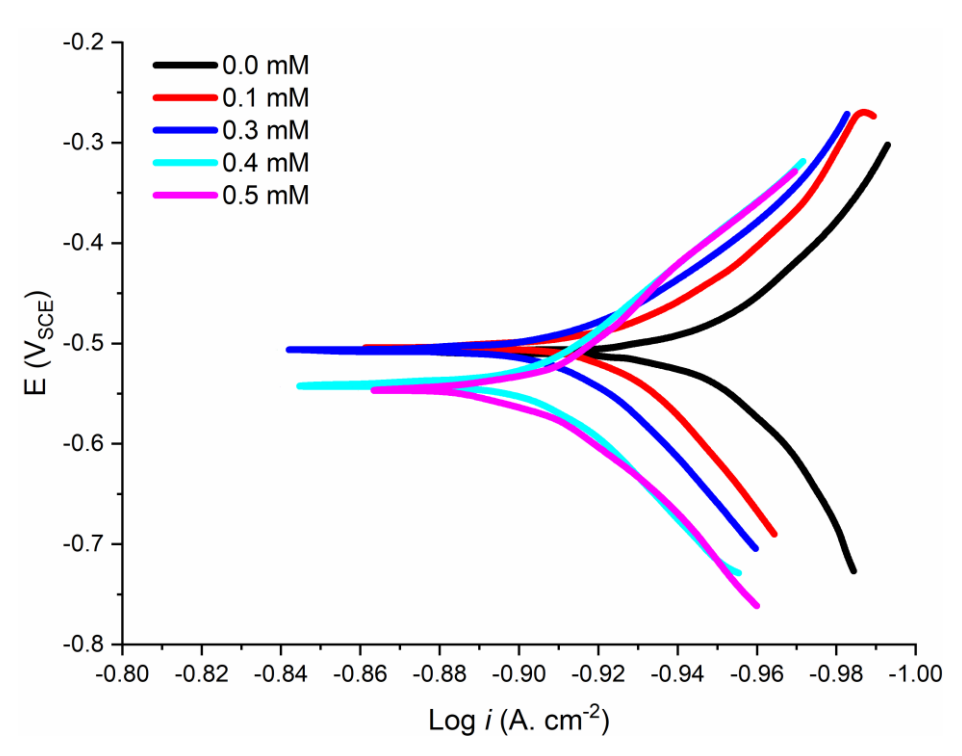


Figure 3. Potentiodynamic polarization curves for mild steel in 1 M HCl with different PBPB concentrations at 303 K.

Table 2. Tafel polarization parameters for mild steel in 1 M HCl with various PBPB concentrations at 303 K.

Conc. (mM)	-E _{corr} (V)	β _a (V·dec ⁻¹)	β _c (V·dec ⁻¹)	i _{corr} (μA·cm ⁻²)	$C_{\rm R} ({\rm mm \cdot y^{-1}})$	IE%
0.0	0.555	5.258	5.128	1.246	11.245	0
0.1	0.560	4.110	5.112	0.616	4.136	50.56
0.3	0.558	4.846	4.916	0.285	2.715	77.12
0.4	0.554	5.104	5.053	0.211	2.165	83.06
0.5	0.547	4.663	4.882	0.172	1.521	87.79

The Tafel polarization parameters provide additional insights into the effectiveness of PBPB as a corrosion inhibitor. values exhibit neglectable changes when the inhibitor concentration is enhanced, and remain around -0.55 V vs. SCE. This constancy reinforces the fact that adding PBPB to the system will not make any contribution to changing the overall electrochemical potential of the system to a great extent, hence its behavior as a mixed-type inhibitor is highly likely [28]. The corrosion i_{corr} also shows a sharp decline with the increasing concentration of PBPB, decreasing from 1.246 μ A/cm² for the blank to 0.172 μ A/cm² at the highest concentration of 0.5 less. This decrease in i_{corr} corresponds to a notable reduction in the corrosion rate which is significant, decreasing from 11.245 mm/year to 1.521 mm/year. This highlights the strong capacity of the inhibitor to inhibit the corrosion process in terms of the change in corrosion current since inhibitor has a significant effect on

the corrosion rate. The greater the concentration of PBPB, the larger the inhibition efficiency (*IE*%) becomes; it peaks at 87.79% for 0.5 mM. Remedial and preventive measures have shown benefit in other similar steel surfaces because corrosion retardation, *i.e.* the degradation of mild steel can be partially slowed. The inhibition efficiency is very high at 0.5 mM due to the building of an involved surface layer on the mild steel with both anodic and cathodic corrosion reactions suppressed. The Tafel plots and the polarization curves confirm that PBPB is an active corrosion inhibitor that suppresses the mechanisms of anodic and cathodic corrosion in the medium of 1 M HCl. With about 87.79% being the maximum extension of the protection provided by PBPB and lies with HCl corrosion, there is potentially higher application of this material to industries that employ corrosion control where corrosion is produced under low pH conditions.

3.3. Comparative discussion: weight loss measurements vs. potentiodynamic polarization measurements

Weight loss and potentiodynamic polarization measurements demonstrated the ability of PBPB as an anti-corrosion inhibitor. Weight loss data showed a decrease in corrosion rate with increasing inhibitor concentration, reaching 91.3% efficiency at 0.5 mM. A slight increase in inhibition efficiency with temperature suggested chemisorption involvement. Polarization measurements confirmed PBPB as a mixed-type inhibitor, reducing both anodic and cathodic reactions, with a maximum efficiency of 87.79% at 0.5 mM. While weight loss provided long-term insights, polarization clarified electrochemical behavior, collectively confirming PBPB's strong protective performance for mild steel in acidic environments [29, 30].

3.4. Adsorption isotherm analysis of PBPB

In this respect, numerous adsorption isotherm models were considered, including Langmuir, Temkin, Frumkin and Freundlich isotherms since all the above mentioned adsorption isotherms conveniently help in the explanation of the mechanism that is responsible for the equilibrium attained between the adsorbed species and the absorbed weak on the metal surface. Progressive regular weight loss measurements followed by modeling the experimental data obtained according to each of the above-listed isotherms in which the inhibitor was in contact with the mild steel will allow the evaluation of relevant thermodesorption parameters and fraction specific methods of treating the inhibitive ability of the contact with the margin. The level of fitting was externally monitored based on the coefficient of determination (R^2) which stands for the adequacy of the fitted model to the data that R^2 that was mentioned previously, [31]. Of the models considered, the Langmuir isotherm provided a higher value of R^2 (0.986) than the other models, which suggest that this model gave the most accurate abstraction of the adsorption process of this compound on steel. This was followed by the Temkin ($R^2 = 0.981$), Frumkin ($R^2 = 0.977$) and Freundlich $(R^2=0.960)$ isotherms. This result also implies the superiority of the Langmuir model in describing the adsorption of PBPB molecules on the mild steel surface investigated in this

study. The role of these two aspects must be understood; it is important to realize that the effect of inhibitors is not complete without adsorption. For the sake of this particular research, the following two equations were employed in order to assess the adsorption characteristics of PBPB on 1 M HCl solution-treated mild steel: The mechanisms presented herein by the other authors as well as the weight loss data served as the basis for the two isotherms formation regarding the adsorption of the inhibitor, as is evident from the given Figure 4, hence giving useful assessments of the efficiency of the inhibitor in protecting the metal surface. The adsorption of proflavine hydrochloride onto activated carbon is best modeled by Langmuir's isotherm which is given by Equation (9):

$$\frac{C_{\rm inh}}{\theta} = \frac{1}{K_{\rm ads}} + C_{\rm inh} \tag{9}$$

where C_{inh} is the concentration, θ is the surface coverage, and K_{ads} is the adsorption equilibrium constant.

In this model, a plot of C_{inh}/θ versus C_{inh} should yield a straight line, with the slope equal to 1 and the intercept corresponding to $1/K_{\rm ads}$. The linearity of the plot and the proximity of the slope to unity indicate that the adsorption of PBPB on the mild steel surface follows the Langmuir isotherm [33]. Figure 4 shows the linearity of the plot, with an R^2 value of 0.986, suggests that the adsorption of PBPB on mild steel follows the Langmuir isotherm closely, indicating a monolayer adsorption on a homogenous surface with no interaction between adsorbed molecules. The slope of the plot (0.807) is close to unity, further confirming the applicability of the Langmuir model to this system. A slope less than 1 suggests a slight deviation from ideal Langmuir behavior, which may be due to interactions between adsorbed inhibitor molecules or surface heterogeneity. However, the high R^2 value indicates that these deviations are minor and do not significantly affect the overall adsorption behavior. The intercept of the plot is 0.134, which corresponds to the inverse of the adsorption equilibrium constant K_{ads} . A higher K_{ads} (7.463 L/mol) value implies stronger adsorption of the inhibitor on the metal surface, leading to more effective corrosion inhibition [34]. The calculated adsorption constant indicates a strong affinity of PBPB for the mild steel surface, contributing to its high inhibition efficiency.

The adsorption isotherm analysis confirms that PBPB adsorbs onto the mild steel surface following the Langmuir isotherm model, forming a monolayer of inhibitor molecules that effectively protect the metal from corrosion. The strong adsorption, indicated by the high R^2 value and appropriate slope, underlines the inhibitor's potential for industrial applications where long-term protection of mild steel in acidic environments is required.

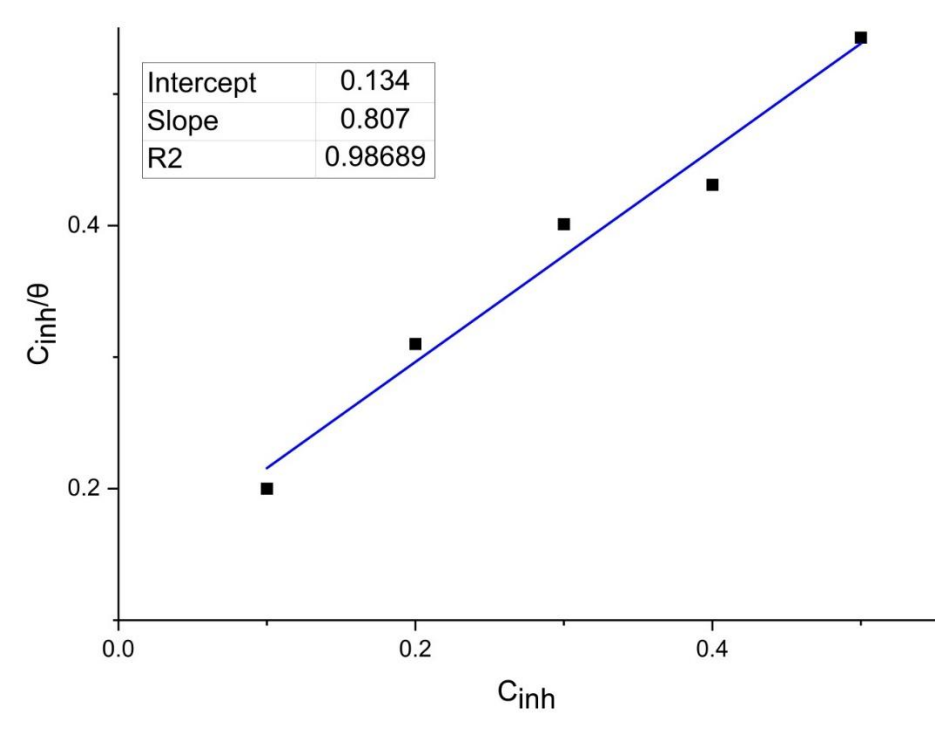


Figure 4. The Langmuir isotherm model.

Moreover, the spontaneity of adsorption and the nature of bonding with the metallic surface were addressed using Gibbs free energy, ΔG , according to the Equation (10):

$$\Delta G_{\text{ads}}^{0} = -RT \ln(55.5K_{\text{ads}})$$
(10)
$$(R=8.314 \text{ J} \cdot \text{mol}^{-1} \cdot \text{K}^{-1}, T=303.15 \text{ K}, [\text{H}_{2}\text{O}]=55.5 \text{ mol} \cdot \text{L}^{-1})$$

The calculated value of $\Delta G_{\rm ads}^0$ is approximately -15.18 kJ. The negative value of $\Delta G_{\rm ads}^0$ signifies that the adsorption of PBPB onto the mild steel surface is a spontaneous process. Additionally, the exothermic nature of the adsorption is implied by the negative sign, indicating that energy is released when inhibitor molecules adhere to the metal surface [35]. The magnitude of $\Delta G_{\rm ads}^0$ provides insights into the type of adsorption. When $\Delta G_{\rm ads}^0$ is less negative than -20 kJ/mol, the adsorption is associated with physisorption, involving weaker van der Waals forces. Values more negative than -40 kJ/mol indicate chemisorption, characterized by the formation of stronger chemical bonds. In this study, $\Delta G_{\rm ads}^0$ value of -15.18 kJ/mol suggests a combined mechanism of physisorption and chemisorption. This supports the formation of a protective monolayer on the mild steel surface, which effectively inhibits corrosion. The strong interaction between the inhibitor molecules and the metal surface is further corroborated by the high $K_{\rm ads}$, reinforcing PBPB's effectiveness as a corrosion inhibitor.

3.5. DFT: quantum chemical parameters calculation

The ionization potential represents the molecule's tendency to lose electrons. A lower value indicates that the molecule can donate electrons more easily, facilitating the formation of strong bonds with the metal surface. The calculated value of 8.560 eV, as shown in Table 3, suggests that PBPB has a moderate tendency to donate electrons, contributing to its adsorption onto the mild steel surface and its inhibitory efficiency [36]. The electron affinity reflects the molecule's ability to accept electrons. With a calculated value of 1.155 eV, PBPB exhibits a capacity to accept electrons from the metal surface, enhancing the stability of the adsorbed protective layer [37]. Electronegativity measures a molecule's ability to attract electrons. PBPB's calculated electronegativity of 4.8575 eV indicates moderate electronattracting power, enabling it to interact effectively with the metal surface. This dual ability to donate and accept electrons strengthens its inhibitory action. Hardness quantifies a molecule's resistance to polarization or deformation of its electron cloud. PBPB's calculated hardness of 3.7025 eV suggests moderate reactivity, striking a balance between molecular stability and its ability to adsorb onto the mild steel surface. Softness (σ) is the inverse of hardness and indicates the molecular reactivity. A higher softness value means that the molecule is more reactive. The softness of 0.2702 eV⁻¹ suggests that PBPB is reactive enough to form a strong protective layer on the mild steel surface [38]. The negative value of ΔN indicates that electrons transfer from the mild steel surface (iron) to the inhibitor. This result aligns with the inhibitor's ability to accept electrons through its LUMO, stabilizing the adsorption process. The magnitude of ΔN supports the strong adsorption ability of PBPB, as both charge donation and acceptance contribute to forming a stable protective layer. [22, 39].

Table 3. Quantum chemical parameters of PBPB.

Parameter	Value
Ionization potential (I)	8.560 eV
Electron affinity (A)	1.155 eV
$E_{ m HOMO}$	$-8.560 \mathrm{eV}$
$E_{ m LUMO}$	−1.155 eV
Electronegativity (χ)	4.8575 eV
Hardness (η)	3.7025 eV
Softness (σ)	$0.2702~{ m eV^{-1}}$
ΔN	-0.0483

Figure 5 shows the optimized structure, E_{HOMO} , and E_{LUMO} of PBPB. These molecular orbitals provide insights into the reactivity and interaction of the inhibitor with the metal surface. The E_{HOMO} represents the orbital from which electrons are most easily donated.

 $E_{\rm HOMO}$ is predominantly localized on the benzene ring and nitrogen atoms in the piperazine ring, indicating that these areas are the most reactive and likely to interact with the metal surface. Electron-donating groups play a critical role in corrosion inhibition by enhancing molecular interactions with the metal surface. The ability of metals to shield equipment from rust and corrosion damage is essential for improving their longevity. Understanding how molecular properties influence corrosion inhibition performance is crucial for optimizing inhibitor efficiency [40]. Moreover, the other important values, E_{HOMO} , and E_{LUMO} will be distributed over bromine and the benzene ring. These values serve as the primary sites from which electrons can be accepted and this is important for enhancing the degree of inhibition, as electrons accepted are crucial to stabilize the layer of inhibitor that has been adsorbed on the metal. Achievement, confirmation as effective corrosion inhibitor of these of quantum chemical parameters and from the DFT simulations. Of these, the hydrogen-rich isomer of the above compound lacks dual properties and this substantiates the fact that more of it is activated Adsorbed inhibitors tend to form stable layers. In addition, softness, hardness and ΔN within medium range may be viewed as providing grounds for PBPB effectiveness of metal/engine interaction for the purpose of inhibition. This is further supported by very high energy barrier to adsorption (very strong adsorption) as evidenced of the negative $\Delta G_{
m ads}^0$ value will render it appropriate for use in some industrial application where prevention of corrosion is in real need.

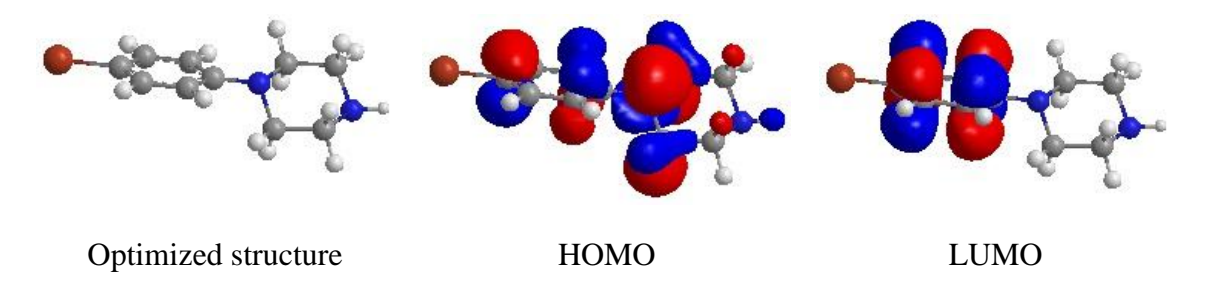


Figure 5. Optimized PBPB molecular structure, E_{HOMO} , and E_{LUMO} orbitals obtained from DFT simulations.

The energy gap between the E_{HOMO} , and E_{LUMO} is a key quantum chemical parameter that reflects the reactivity and stability of a molecule. This gap (ΔE) is inversely proportional to molecular reactivity: a smaller ΔE indicates higher reactivity, enabling easier electron transfer to or from the surroundings, which enhances interaction with the metal surface. Conversely, a larger ΔE signifies lower reactivity and greater molecular stability. In the case of PBPB, the calculated energy gap of 7.405 eV is relatively large, suggesting that the molecule is stable while maintaining moderate reactivity. This stability allows PBPB to interact effectively with the mild steel surface without undergoing significant structural changes, making it suitable for long-term corrosion protection. A larger energy gap also indicates that the inhibitor is less prone to disruption during adsorption, ensuring it maintains its protective integrity over time. While a smaller ΔE typically facilitates stronger adsorption

by promoting electron transfer, PBPB's well-distributed $E_{\rm HOMO}$, and $E_{\rm LUMO}$ across its structure enable effective electron donation and acceptance. This distribution supports strong adsorption onto the mild steel surface, even with a relatively large energy gap. ΔE also sheds light on the mechanism of adsorption. Molecules with smaller ΔE are more likely to form stronger chemical bonds, indicative of chemisorption. In contrast, the relatively large ΔE of PBPB suggests that physisorption – characterized by weaker, physical adsorption – plays a significant role alongside chemisorption. This dual mechanism helps form a stable and effective protective layer on the mild steel surface. In summary, the energy gap of 7.405 eV demonstrates that PBPB is a stable and moderately reactive inhibitor. Its balanced ability to donate and accept electrons, as reflected by its $E_{\rm HOMO}$ and $E_{\rm LUMO}$ distributions, enables efficient interaction with the mild steel surface. This balance underpins its success as a corrosion inhibitor, with both physisorption and chemisorption contributing to a robust protective layer.

The protonation of the PBPB molecule: Another analysis from the optimization arguments for protonated PBPB of the electronic and geometric structure of the physisorbed complex and its reactions. Upon the above discussion, we come to piperazine rings. It contains nitrogen atoms for dendying, and type of interaction between the 15% nitrogen atom in positive protonated condition 16 and piperazine ring distinctly, and gently observe that located nitrogen atom piperazine 17 pendant ring undergoes slight changes to adjust to the positive charge satisfying the required angle keeping stability of piperazine ring, but producing the reactive layer on the metal with such system. The positively charged piperazine ring has an increased electric charge density which also helps it to accept the incoming, the free electrons, promote its adsorption on the negatively charged steel surface. The $E_{\rm HOMO}$ diagrammed as in the Figure 6 explicates the electron distribution in the protonated PBPB molecule, both in density and extent. The E_{HOMO} is localized per the piperazine nitrogen atoms and the benzene ring right above it, then its affinity with the benzene ring is regarding normal aromaticity established there. The variation in charge distribution suggests the presence of different charge states and protonation effects, influencing the inhibitor's electronic properties and adsorption behavior. Protonation in the piperazine unit lowers E_{HOMO} energy level, reducing the molecule's ability to donate electrons compared to its non-protonated form. While protonation reduces electron donation, it enhances the molecule's ability to accept electrons via the LUMO, which improves its interaction with the metal surface and strengthens adsorption. The $E_{\rm HOMO}$ field of the molecule similar to what is plotted in the Figure 6 also gives directions on the areas of the molecule which are able to receive electrons. Generated E_{LUMO} is fairly scattered within the bromine atom and the benzene, if air view is unconstitutional then these regions are feasible electron addition deposits during metal adsorption reactions. Protonation lowers E_{LUMO} level, increasing the molecule's ability to accept electrons, thereby enhancing its adsorption efficiency on the metal surface.

Protonation increases the molecule's capability to adsorb on the mild steel surface due to reduced charge strength. This leads to stronger interactions between the inhibitor and the

metal surface, improving corrosion protection. The protonated structure maintains sufficient π -electron density on the benzene ring, supporting initial weak adsorption via van der Waals forces. The positively charged nitrogen in the piperazine ring facilitates stronger chemisorptive interactions with the negatively charged sites on the mild steel surface, forming a durable protective layer. The shift in $E_{\rm HOMO}$ and $E_{\rm LUMO}$ levels upon protonation ensures an optimal balance between electron donation and acceptance, maximizing the efficiency of the dual adsorption mechanism.

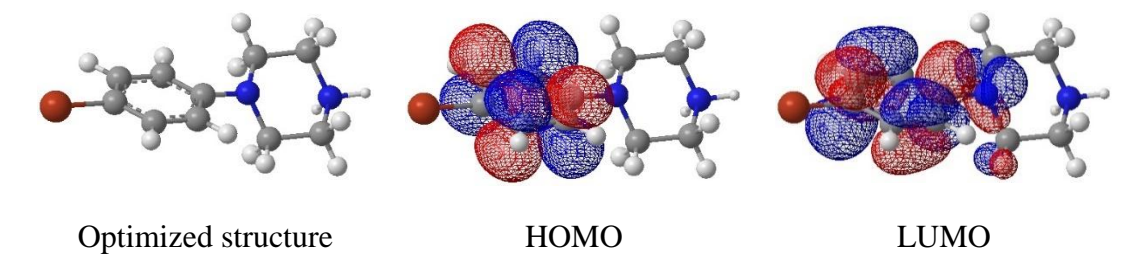


Figure 6. Optimized molecular structure, E_{HOMO} , and E_{LUMO} orbitals of protonated PBPB molecule obtained from DFT simulations.

Ionization Potential indicates the energy required to remove an electron from the molecule. A lower value (1.150 eV) suggests that the molecule can easily donate electrons, facilitating strong adsorption through its $E_{\rm HOMO}$ sites. Electron Affinity (A), reflects the molecule's ability to accept electrons (Table 4). The negative value (-1.780 eV) implies a reduced tendency to accept electrons, likely due to protonation redistributing the electron density. Electronegativity (χ) calculated value of -0.315 eV reflects the overall electronic pull of the molecule. The negative value indicates a shift in the molecule's electron density balance due to protonation, making it more reactive with electron-dense regions of the metal surface. Hardness (η) is a measure of the molecule's resistance to deformation or polarization. The value (1.465 eV) suggests moderate stability, allowing the molecule to effectively interact with the metal surface without excessive reactivity. σ is the inverse of hardness. A value of 0.683 eV $^{-1}$ suggests that the molecule is sufficiently reactive to form strong bonds with the mild steel surface, enhancing corrosion inhibition. ΔN indicates the molecule's ability to accept electrons from the metal. The value of 0.034 eV is low, reflecting the dominant role of electron donation in the adsorption process.

Table 4. Quantum chemical parameters of protonated PBPB molecule.

Parameter	Value
I	1.150 eV
A	$-1.780~\mathrm{eV}$
$E_{ m HOMO}$	$-1.150 \mathrm{eV}$
$E_{ m LUMO}$	1.780 eV

Parameter	Value	
χ	−0.315 eV	
η	1.465 eV	
σ	$0.683~{\rm eV^{-1}}$	
ΔN	0.034	

3.6. Atomic charges of PBPB

The atomic charges of a molecule provide crucial insights into the distribution of electron density across different atoms, which in turn influences the molecule's reactivity, interaction with other species, and overall chemical behavior. The atomic charges of the PBPB inhibitor, as shown in Figure 7, reveal significant details about the potential sites for interaction with the mild steel surface. The nitrogen atoms in the piperazine ring carry the most negative charges in the molecule, with N(4) –0.9 being slightly more negative than N(1) –0.8382. These highly negative charges indicate a high electron density around the nitrogen atoms, making them the primary sites for nucleophilic attack. In the context of corrosion inhibition, these nitrogen atoms are likely to interact strongly with the positively charged iron atoms on the mild steel surface, forming stable coordination bonds. This interaction plays a critical role in the chemisorption process, contributing significantly to the formation of a protective layer on the metal surface. The carbon atoms in the piperazine ring exhibit a range of charges, with C(2) - 0.411 being more negative, while C(3) 0.27 and C(5) 0.27 are positively charged. The negative charge on C(2) suggests it might also participate in weak interactions with the metal surface, although its contribution would be secondary compared to the nitrogen atoms. The positive charges on C(3), C(5), and C(6) 0.3691 suggest these atoms are less likely to directly interact with the metal surface but instead influence the overall electronic environment of the nitrogen atoms, further enhancing their reactivity. The carbon atoms in the benzene ring show a mixture of positive and negative charges, indicating an uneven distribution of electron density. The presence of negative charges on C(8), C(9), C(11), and C(12) [Charge: C(8): -0.153; C(9): -0.15; C(10): 0.111; C(11): -0.157 and C(12): -0.147] suggests potential sites for weak interactions, possibly contributing to physisorption on the mild steel surface. However, the benzene ring is more likely to be involved in van der Waals interactions rather than strong chemical bonding, indicating its role in physisorption rather than chemisorption. The bromine atom [Br(13): -0.111] despite its relatively low negative charge compared to the nitrogen atoms, still contributes to the molecule's overall electron density. The bromine atom's electronegativity and position in the para location relative to the piperazine ring suggest it plays a role in stabilizing the electronic structure of the molecule. While it might not directly participate in strong interactions with the metal surface, it helps maintain the molecule's overall geometry and electron distribution, which can influence the effectiveness of the inhibitor [41]. The PBPB atomic charges distribution

suggests some main points illustrating the inhibitory action effectiveness towards the corrosion process:

- Mainly, the N atoms which have large negative charge are sites for chemisorption and do undergo coordination interaction to metals from Br atoms. The chemisorption is crucial in making a stable protection layer that prevents corrosion of mild steel in an acidic environment.
- Chemical grifts that carbon atoms in the benzene ring also the bromine help the substance to physiosorbed onto the metal surface while with weaker forces but once the inhibitor is introduced in the corrosive media, these interactions make a first barrier that grow rapidly.
- The charges mainly from other carbon atoms in piperazine and benzene rings in addition to the corresponding charges in bromine, are for keeping the molecule's quality and shape of its structure. This is a vital characteristic because such coverage effectively prevents and ameliorates the propensity of corrosion agents to attack the metal substrates.

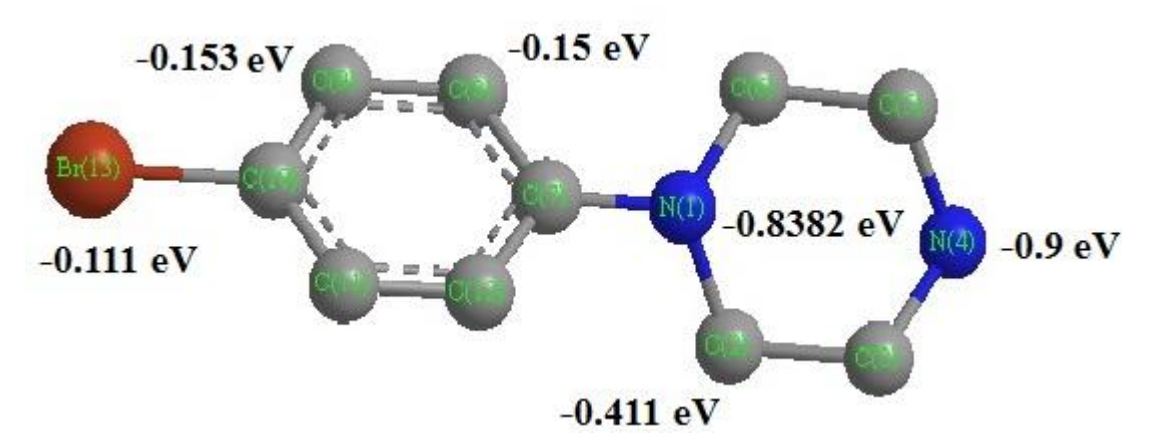


Figure 7. The atomic charges foe the tested inhibitor molecule.

3.7. Suggested inhibition mechanism for PBPB on mild steel

The proposed inhibition mechanism for PBPB on the mild steel surface involves a dual physisorption and chemisorption adsorption process which were effectively shielding the steel from HCl. This combination of mechanisms ensures both rapid initial adsorption and long-term stability, contributing to the high inhibition efficiency observed in experimental results. Physisorption occurs when PBPB molecules interact with the mild steel surface through weak van der Waals forces. The bromine atom in the para position of the benzene ring, along with the π -electron-rich regions of the benzene ring, contributes to the physisorption process. These interactions, though reversible and relatively weak, provide a quick initial protective barrier over the metal surface. The physisorption process can be represented as

 $Inhibitor_{sol} \rightleftharpoons Inhibitor_{ads}^{physisorption}$

In the present context, Inhibitor_{sol} represents the PBPB molecules in solution, and Inhibitor^{physisorption} represents the PBPB molecules adsorbed on the mild steel surface via physisorption.

Chemisorption is characterized by the existence of much stronger and more stable bonds which are formed between the PBPB molecules and the mild steel. Such covalent-like bond is formed due to a Presentation the non-bonding pairs of d-orbital electrons of Fe with the nitrogen atoms in the piperazine ring and it ensures that a stable, self-limiting protective layer regardless of a varying high temperatures or imbalanced acid solution distributions on steel is formed. The chemisorption progress can be formulated in the following reaction:

$$Fe + Inhibitor^{physisorption}_{ads} \rightleftharpoons Fe - Inhibitor^{physisorption}_{ads}$$

In this case, Fe represents the iron atoms present on the mild steel and the term Fe–Inhibitor^{physisorption} chemisorbed PBPB on the mild steel surface [44].

At first, PBPB molecules conform to the metal surface and easily undergo adsorption through physical adsorption, which results in a first formed but limited corrosion protection. As the time proceeds, the more stable forces of chemical bonds (adsorption) prevail and such a protection becomes stable and can withstand severe conditions. The PBPB in this case, can benefit from this dual adsorption process where it forms a proper barrier, a number of layers have formed on the surface of the mild steel which subcludes the PBPB from any interaction with the mild steel substrate. The interaction between PBPB and the mild steel proceeds through the coupled action of the two mechanisms described in the following:

$$Fe_{surface} + Inhibitor_{solution} \rightarrow Fe - Inhibitor_{ads}$$

Physisorption provides rapid or instant effective surface coverage on mild steel and hence does not enhance the corrosion, process that includes corrosion. Chemisorption, as a technique, secures corrosion prevention over a long period since it generates a particularly firm chemical bonding. Both ways of using the inhibitors elevate the effect of inhibition, guaranteeing the most efficient coverage.

Conclusion

This study investigated the corrosion inhibition efficiency of PBPB for mild steel in an acidic medium using weight loss measurements, potentiodynamic polarization, and DFT simulations. The key findings are as follows:

- 1. PBPB demonstrated significant inhibition efficiency, reaching 91.3% in weight loss measurements and 87.79% in polarization studies at 0.5 mM concentration, effectively mitigating both anodic and cathodic corrosion processes.
- 2. The slight increase in inhibition efficiency with temperature observed in weight loss studies indicates robust performance under elevated thermal conditions, likely due to chemisorption strengthening at higher temperatures.

- 3. PBPB adsorption followed the Langmuir isotherm, confirming monolayer formation. The negative Gibbs free energy highlighted the spontaneous and exothermic nature of the process, driven by a combination of physisorption and chemisorption.
- 4. DFT simulations identified nitrogen atoms in the piperazine ring as primary sites for chemisorption, supported by a moderate energy gap (ΔE =7.405 eV), indicating a balance between stability and reactivity.
- 5. The synergistic combination of initial physisorption and subsequent chemisorption ensures rapid surface coverage and long-term stability, forming a durable protective layer on mild steel.

The study underscores the potential of PBPB as an effective corrosion inhibitor for industrial applications in acidic environments. Its ability to form a stable, dual-layer protective mechanism and its consistent performance across varying temperatures make it a promising candidate for mitigating corrosion in harsh conditions.

Conflict of Interest

The Authors declare that no Conflict of Interest.

Funding Declaration

This research was funded by Al-Ayen Iraqi University (AUIQ) under the program "Innovative Corrosion Inhibitors: A New Frontier in Materials Protection" (AUIQ-RFP-2024-CI). The authors express their sincere gratitude for the financial support that made this study possible.

Acknowledgment

The authors would like to express their heartfelt gratitude to Al-Ayen Iraqi University (AUIQ) for providing the financial support under the research project titled "Innovative Corrosion Inhibitors: A New Frontier in Materials Protection" (Project Code: AUIQ-RFP-2024-CI). Their assistance and resources were invaluable in the successful completion of this study.

Data Availability

The data supporting the findings of this study are available within the manuscript. Additional data may be available upon request from the corresponding author.

References

1. F. Zhang, Y. Tang, Z. Cao, W. Jing, Z. Wu and Y. Chen, Performance and theoretical study on corrosion inhibition of 2-(4-pyridyl)-benzimidazole for mild steel in hydrochloric acid, *Corros. Sci.*, 2012, **61**, 1–9. doi: 10.1016/j.corsci.2012.03.045

- 2. A.M. Resen, M.M. Hanoon, W.K. Alani, A. Kadhim, A.A. Mohammed, T.S. Gaaz, A.A.H. Kadhum, A.A. Al-Amiery and M.S. Takriff, Exploration of 8-piperazine-1-ylmethylumbelliferone for application as a corrosion inhibitor for mild steel in hydrochloric acid solution, *Int. J. Corros. Scale Inhib.*, 2021, **10**, no. 1, 368–387. doi: 10.17675/2305-6894-2021-10-1-21
- 3. A.J.M. Eltmimi, A. Alamiery, A.J. Allami, R.M. Yusop, A.H. Kadhum and T. Allam, Inhibitive effects of a novel efficient Schiff base on mild steel in hydrochloric acid environment, *Int. J. Corros. Scale Inhib.*, 2021, **10**, no. 2, 634–648. doi: 10.17675/2305-6894-2021-10-2-10
- 4. A. Alamiery, W.N.R.W. Isahak, H. Aljibori, H. Al-Asadi and A. Kadhum, Effect of the structure, immersion time and temperature on the corrosion inhibition of 4-pyrrol-1-yl-*N*-(2,5-dimethyl-pyrrol-1-yl)benzoylamine in 1.0 M HCl solution, *Int. J. Corros. Scale Inhib.*, 2021, **10**, no. 2, 700–713. doi: 10.17675/2305-6894-2021-10-2-14
- 5. M.M. Solomon, I.E. Uzoma, J.A.O. Olugbuyiro and O.T. Ademosun, A Censorious Appraisal of the oil well acidizing corrosion inhibitors, *J. Pet. Sci. Eng.*, 2022, **215**, 110711. doi: 10.1016/j.petrol.2022.110711
- 6. A.A. Altalhi, Anticorrosion Investigation of New Diazene-Based Schiff Base Derivatives as Safe Corrosion Inhibitors for API X65 Steel Pipelines in Acidic Oilfield Formation Water: Synthesis, Experimental, and Computational Studies, *ACS Omega*, 2023, **8**, no. 34, 31271–31280. doi: 10.1021/acsomega.3c03592
- 7. T.A. Salman, A.A. Al-Amiery, L.M. Shaker, A.A.H. Kadhum and M.S. Takriff, A study on the inhibition of mild steel corrosion in hydrochloric acid environment by 4-methyl-2-(pyridin-3-yl)thiazole-5-carbohydrazide, *Int. J. Corros. Scale Inhib.*, 2019, **8**, no. 4, 1035–1059. doi: 10.17675/2305-6894-2019-8-4-14
- 8. B.D.B. Tiu and R.C. Advincula, Polymeric Corrosion Inhibitors for the Oil and Gas Industry: Design Principles and Mechanism, *React. Funct. Polym.*, 2015, **95**, 25–45. doi: 10.1016/j.reactfunctpolym.2015.08.006
- 9. F.F. Sayyid, S.I. Ibrahim, M.M. Hanoon, A.A.H. Kadhum and A.A. Al-Amiery, Gravimetric Measurements and Theoretical Calculations of 4-Aminoantipyrine Derivatives as Corrosion Inhibitors for Mild Steel in Hydrochloric Acid Solution: Comparative Studies, *Corros. Sci. Technol.*, 2023, **22**, no. 2, 73–89. doi: 10.14773/CST.2023.22.2.73
- 10. M. Farsak, H. Keleş and M.A. Keleş, A new corrosion inhibitor for protection of low carbon steel in HCl solution, *Corros. Sci.*, 2015, **98**, 223–232. doi: 10.1016/j.corsci.2015.05.036
- 11. S. Jagadeesan, F. Benhiba, A. Nagarajan, A. Zarrouk and S. Chitra, Thiazolo thiadiazole derivatives as anti-corrosion additives for acid corrosion, *Chem. Data Collect.*, 2020, **26**, no. 4, 100358. doi: 10.1016/j.cdc.2020.100358
- 12. P. Muthukrishnan, B. Jeyaprabha and P. Prakash, Adsorption and corrosion inhibiting behavior of *Lannea coromandelica* leaf extract on mild steel corrosion, *Arabian J. Chem.*, 2017, **10**, S2343–S2354. doi: 10.1016/j.arabjc.2013.08.011

- 13. B. Hammouti, A. Zarrouk, S.S. Al-Deyab and I. Warad, Temperature Effect, Activation Energies and Thermodynamics of Adsorption of Ethyl-2-(4-(2-ethoxy-2-oxoethyl)-2-ptolylquinoxalin-1(4*H*)-yl)acetate on Cu in HNO₃, *Orient. J. Chem.*, 2011, **27**, no. 1, 23–31.
- 14. E.A. Noor and A.H. Al-Moubaraki, Thermodynamic study of metal corrosion and inhibitor adsorption processes in mild steel/1-methyl-4[4'-(-X)-styryl pyridinium iodides/hydrochloric acid systems, *Mater. Chem. Phys.*, 2008, **110**, no. 1, 145–154. doi: 10.1016/j.matchemphys.2008.01.028
- 15. K. Vignesh, S. Sujithra, M. Vajjiravel, J. Narenkumar, B. Das, M.S. AlSalhi, S. Devanesan, A. Rajasekar and T. Malik, Synthesis of novel N-substituted tetrabromophthalic as corrosion inhibitor and its inhibition of microbial influenced corrosion in cooling water system, *Sci. Rep.*, 2024, **14**, 25408. doi: 10.1038/s41598-024-76254-8
- 16. H.S. Aljibori, A.H. Alwazir, S. Abdulhadi, W.K. Al-Azzawi, A.A.H. Kadhum, L.M. Shaker, A.A. Al-Amiery and H.Sh. Majdi, The use of a Schiff base derivative to inhibit mild steel corrosion in 1 M HCl solution: a comparison of practical and theoretical findings, *Int. J. Corros. Scale Inhib.*, 2022, **11**, no. 4, 1435–1455. doi: 10.17675/2305-6894-2022-11-4-2
- 17. ASTM International, *Standard Practice for Preparing*, *Cleaning*, and *Evaluating Corrosion Test*, 2011, 1–9.
- 18. NACE International, Laboratory Corrosion Testing of Metals in Static Chemical Cleaning Solutions at Temperatures below 93°C (200°F), TM0193-2016-SG, 2000.
- 19. E. McCafferty, Validation of corrosion rates measured by Tafel extrapolation method, *Corros. Sci.*, 2005, **47**, no. 12, 3202–3215. doi: 10.1016/j.corsci.2005.05.046
- 20. M.J. Frisch, G.W. Trucks, H.B. Schlegel, G.E. Scuseria, M.A. Robb, J.R. Cheeseman, J.A. Montgomery, Jr., T. Vreven, K.N. Kudin, J.C. Burant, J.M. Millam, S.S. Iyengar, J. Tomasi, V. Barone, B. Mennucci, M. Cossi, G. Scalmani, N. Rega, G.A. Petersson, H. Nakatsuji, M. Hada, M. Ehara, K. Toyota, R. Fukuda, J. Hasegawa, M. Ishida, T. Nakajima, Y. Honda, O. Kitao, H. Nakai, M. Klene, X. Li, J.E. Knox, H.P. Hratchian, J.B. Cross, V. Bakken, C. Adamo, J. Jaramillo, R. Gomperts, R.E. Stratmann, C. Pomelli, R. Cammi, J.W. Ochterski, O. Yazyev, A.J. Austin, P.Y. Ayala, K. Morokuma, G.A. Voth, P. Salvador, J.J. Dannenberg, V.G. Zakrzewski, S. Dapprich, A.D. Daniels, M.C. Strain, O. Farkas, D.K. Malick, A.D. Rabuck, K. Raghavachari, J.V.Ortiz, Q. Cui, A.G. Baboul, S. Clifford, J.B. Foresman, J. Cioslowski, B.B. Stefanov, G. Liu, A. Liashenko, P. Piskorz, I. Komaromi, R.L. Martin, D.J. Fox, T. Keith, M.A. AlLaham, C.Y. Peng, A. Nanayakkara, M. Challacombe, P.M.W. Gill, B. Johnson, W. Chen, M.W. Wong, C. Gonzalez and J.A. Pople, Gaussian 03, Revision B.05, Gaussian, Inc., Wallingford CT, 2004.
- 21. T. Koopmans, Ordering of wave functions and eigen-energies to the individual electrons of an atom, *Physica*, 1934, 1, no. 1–6, 104-113 (in German). doi: 10.1016/80031-8914(34)90011-2

- 22. A. Kokalj and N. Kovacevic, On the consistent use of electrophilicity index and HSAB-based electron transfer and its associated change of energy parameters, *Chem. Phys. Lett.*, 2011, **507**, no. 1–3, 181–184. doi: 10.1016/j.cplett.2011.03.045
- 23. A.M. Resen, M.M. Hanoon, W.K. Alani, A. Kadhim, A.A. Mohammed, T.S. Gaaz, A.A.H. Kadhum, A.A. Al-Amiery and M.S. Takriff, Exploration of 8-piperazine-1-ylmethylumbelliferone for application as a corrosion inhibitor for mild steel in hydrochloric acid solution, *Int. J. Corros. Scale Inhib.*, 2021, **10**, no. 1, 368–387. doi: 10.17675/2305-6894-2021-10-1-21
- 24. G. Ji, S. Anjum, S. Sundaram and R. Prakash, *Musa paradisica* peel extract as green corrosion inhibitor for mild steel in HCl solution, *Corros. Sci.*, 2015, **90**, 107–117. doi: 10.1016/j.corsci.2014.10.002
- 25. C. Verma, V.S. Saji, M.A. Quraishi and E.E. Ebenso, Pyrazole derivatives as environmental benign acid corrosion inhibitors for mild steel: Experimental and computational studies, *J. Mol. Liq.*, 2020, **298**, 111943. doi: 10.1016/j.molliq.2019.111943
- 26. M.D. Plotnikova, A.B. Shein, M.G. Scherban, A.N. Vasyanin and A.E. Rubtsov, Experimental and theoretical investigation of (*E*)-5-{[4-(dimethylamino)benzylidene]amino}-1,3,4-thiadiazole-2(3*H*)-thione (DATT) as an acid corrosion inhibitor of mild steel, *Int. J. Corros. Scale Inhib.*, 2023, **12**, no. 4, 1365–1391. doi: 10.17675/2305-6894-2023-12-4-1
- 27. N. Dheer, A.K. Kalra, D. Singh, S.K. Ujjain, P. Ahuja, R. Kumar, P. Singh, N.K. Johar, M.R. Singh and R. Kanojia, Mild steel corrosion inhibition by nicotinamide as a green inhibitor: An electrochemical, thermodynamic and theoretical insight, *Int. J. Corros. Scale Inhib.*, 2023, **12**, no. 4, 1645–1667. doi: 10.17675/2305-6894-2023-12-4-13
- 28. A. Elyoussfi, H. Outada, J. Issad, H. Lrhoul, A. Salhi and A. Dafali, Corrosion inhibitors of alloysand metals in acidic solution: Abibliometric analysis from 2010 to 2022, *Int.J. Corros. Scale Inhib.*, 2023, **12**, no. 2, 722–740. doi: 10.17675/2305-6894-2023-12-2-19
- 29. R.K. Mitra, R. Yadav, A. Tomar and M. Yadav, Computational and experimental evaluation on pyrazoles as corrosion inhibitor in HCl solution: DFT and electrochemical analysis, *Int. J. Corros. Scale Inhib.*, 2024, **13**, no. 4, 1908–1935. doi: 10.17675/2305-6894-2024-13-4-2
- 30. S. Al-Baghdadi, A. Al-Amiery, T. Gaaz and A. Kadhum, Terephthalohydrazide and isophthalo-hydrazide as new corrosion inhibitors for mild steel in hydrochloric acid: Experimental and theoretical approaches, *Koroze Ochr. Mater.*, 2021, **65**, 12–22. doi: 10.2478/kom-2021-0002
- 31. A. Al-Amiery, Anti-Corrosion performance of 2-isonicotinoyl-*N*-phenylhydrazinecarbothioamide for mild steel hydrochloric acid solution: insights from experimental measurements and quantum chemical calculations, *Surf. Rev. Lett.*, 2021, **28**, no. 3, 2050058. doi: 10.1142/S0218625X20500584

- 32. H.K. Thabet, J.M. AlGhamdi, H.A. Mohammed, M.A.M. Elsaid and A.M. Ashmawy, Anticorrosion Agents for Carbon Steel in Acidic Environments: Synthesis and Quantum Chemical Analysis of New Schiff Base Compounds with Benzylidene, *ACS Omega*, 2023, **8**, no. 42, 39770–39782. doi: 10.1021/acsomega.3c05790
- 33. A.G. Sayed, A.M. Ashmawy, W.E. Elgammal, S.M. Hassan and M.A. Deyab, Synthesis, description, and application of novel corrosion inhibitors for CS AISI1095 in 1.0 M HCl based on benzoquinoline derivatives, *Sci. Rep.*, 2023, **13**, no. 1, 13761. doi: 10.1038/s41598-023-39714-1
- 34. S.L.A. Kumar, M. Gopiraman, M.S. Kumar and A. Sreekanth, 2-Acetylpyridine-*N*(4)-morpholine thiosemicarbazone (HAcpMTSc) as a corrosion inhibitor on mild steel in HCl, *Ind. Eng. Chem. Res.*, 2011, **50**, no. 13, 7824–7832. doi: 10.1021/ie200487g
- 35. A.Yu. Luchkin, I.A. Kuznetsov, N.N. Andreev, O.A. Goncharova and S.S. Vesely, Surface layers formed upon chamber treatment of copper with octadecylamine, *Int. J. Corros. Scale Inhib.*, 2024, **13**, no. 3, 1715–1723. doi: 10.17675/2305-6894-2024-13-3-21
- 36. H.M.A. El-Lateef, M.M. Khalaf, K. Shalabi and A.A. Abdelhamid, Efficient synthesis of 6,7-dihydro-5*H*-cyclopenta[b]pyridine-3-carbonitrile compounds and their applicability as inhibitor films for steel alloy corrosion: collective computational and practical approaches, *ACS Omega*, 2022, **7**, no. 28, 24727–24745. doi: 10.1021/acsomega.2c02639
- 37. C. Verma, M.A. Quraishi and K.Y. Rhee, Corrosion inhibition relevance of semicarbazides: electronic structure, reactivity and coordination chemistry, *Rev. Chem. Eng.*, 2022, **39**, no. 6, 1005–1026. doi: 10.1515/revce-2022-0009
- 38. A.M. Mustafa, F.F. Sayyid, N. Betti, L.M. Shaker, M.M. Hanoon, A.A. Alamiery, A.A.H. Kadhum and M.S. Takriff, Inhibition of mild steel corrosion in hydrochloric acid environment by 1-amino-2-mercapto-5-(4-(pyrrol-1-yl)phenyl)-1,3,4-triazole, *S. Afr. J. Chem. Eng.*, 2022, **39**, 42–51. doi: 10.1016/j.sajce.2021.11.009
- 39. M.E. Khabazi and A.N. Chermahini, DFT Study on Corrosion Inhibition by Tetrazole Derivatives: Investigation of the Substitution Effect, *ACS Omega*, 2023, **8**, no. 11, 9978–9994. doi: 10.1021/acsomega.2c07185
- 40. Y. Shi, L. Chen, S. Zhang, H. Li and F. Gao, New branched benign compounds including double antibiotic scaffolds: synthesis, simulation and adsorption for anticorrosion effect on mild steel, *Front. Chem. Sci. Eng.*, 2023, **17**, 167–182. doi: 10.1007/s11705-022-2199-2
- 41. C.U. Ibeji, D.C. Akintayo, H.O. Oluwasola, E.O. Akintemi, O.G. Onwukwe and O.M. Eziomume, Synthesis, experimental and computational studies on the anticorrosion performance of substituted Schiff bases of 2-methoxybenzaldehyde for mild steel in HCl medium, *Sci. Rep.*, 2023, **13**, no. 1, 3265. doi: 10.1038/s41598-023-30396-3

- 42. K.F. Khaled and M.A. Amin, Computational and electrochemical investigation for corrosion inhibition of nickel in molar nitric acid by piperidines, *J. Appl. Electrochem.*, 2008, **38**, no. 11, 1609–1621. doi: 10.1007/s10800-008-9604-5
- 43. P.T. Scaria, P. Shetty, P. Preethi and S. Kagatikar, 2-Aminobenzothiazole as an efficient corrosion inhibitor of AA6061-T6 in 0.5 M HCl medium: electrochemical, surface morphological, and theoretical study, *J. Appl. Electrochem.*, 2022, **52**, 1675–1689. doi: 10.1007/s10800-022-01742-6
- 44. B. El Ibrahimi, A. Jmiai, L. Bazzi and S. El Issami, Amino acids and their derivatives as corrosion inhibitors for metals and alloys, *Arabian J. Chem.*, 2020, **13**, no. 1, 740–771. doi: 10.1016/j.arabjc.2017.07.013
- 45. N.P. Swathi, S. Samshuddin, T.A. Aljohani, K. Rasheeda, V.D.P. Alva, F.Y. Alomari and A.H. Alamri, A new 1,2,4-triazole derivative as an excellent corrosion inhibitor: Electrochemical experiments with theoretical validation, *Mater. Chem. Phys.*, 2022, **291**, 126677. doi: 10.1016/j.matchemphys.2022.126677

*** * ***